[Frontiers In Bioscience, Elite, 11, 79-88, Jan 1, 2019]

Characterization of embryonic cells obtained from multifetal reduction

Ragaa Mansour[1], Mohamed Aboulghar[1,2], Nehal I. Ghoneim[3], Toka A. Ahmed[3], Ahmed El-Badawy[3], Sara M. Ahmed[3], Samaa S. Kamar[4], Maha Baleigh[4], Amal M. Abbas[1,4], Hesham F. Kayed[1,5], Mahmoud Gabr[6], Nagwa El-Badri[3]

[1]The Egyptian IVF-ET Center, 3 Road 161 Hadayek El-Maadi, Cairo 11431, Egypt, [2]Department of Obstetrics and Gynecology, Faculty of Medicine, Cairo University, Cairo, Egypt, [3]Center of Excellence for Stem Cells and Regenerative Medicine (CESC), Zewail City of Science and Technology, Giza, Egypt, [4]Department of Medical Histology and Cell Biology, Faculty of Medicine, Cairo University, Cairo, Egypt, [5]Cytogenetic Department, National Egyptian Research Institute, Cairo, Egypt, [6]The Urology and Nephrology Center, Mansoura University. Mansoura, Egypt

TABLE OF CONTENTS

1. Abstract
2. Introduction
3. Materials and methods
3.1. Materials
3.1.1. Reagents.
3.1.2. Equipment and software
3.2. Methods
3.2.1. Multifetal reduction
3.2.2. Tissue culture
3.2.3. RNA extraction and RT-PCR
3.2.4. Confocal Immunofluorescence Imaging
3.2.5. Histology and immunohistochemistry
3.2.6. Morphometric studies
3.2.7. Cytogenetic analysis
3.2.8. In vivo transplantation
4. Results
4.1. MFR-ECs express human ESCs-related markers
4. 2. Histology and immunohistochemistry
4. 3. Expression of genes related to the three germ layers
4. 4. Low expression levels of cancer-related genes
4. 5. Histochemical analysis
4. 6. In vivo transplantation
5. Discussion
6. Acknowledgements
7. References

1. ABSTRACT

The multifetal reduction (MFR) procedure is usually reserved for high-order multiple pregnancies, and aspirated tissues are typically discarded. In this study, cells obtained from MFR tissue (termed multifetal reduction embryonic cells (MFR-ECs)), were characterized *in vitro* by genotypic and phenotypic analyses and tested *in vivo* by injection under the kidney capsule of nude mice. MFR-ECs were highly proliferative in culture and showed a normal karyotype by microarray CGH. Immunohistochemical analysis at day zero showed positive focal staining for desmin, S-100 protein, synaptophysin and chromogranin. Histology examination showed a mixture of cells from the three germ layers at different stages of differentiation. Markers of these stages included important developmental transcription factors, such as beta three-tubulin (ectoderm), paired box 6 (ectoderm) and alpha-smooth muscle actin (mesoderm). Quantitative polymerase chain reaction (qPCR) showed down-regulation of the mRNAs of cancer-related genes such as TP53. *In vivo* transplantation in nude mice showed a typical

hyaline cartilage plate and no teratoma formation. Thus, MFR-ECs represent a rich, unique source for studying stem cell development, embryogenesis and cell differentiation.

2. INTRODUCTION

The incidence of multifetal pregnancies increased dramatically due to the increased use of Assisted Reproduction Techniques (ART). The high-order triplet or greater birth rate with all its complications increased more than 400% between 1980 and 1996 (1, 2). This rate decreased by 29% between 1998 and 2009 due to a reduction in the number of embryos per transfer in ART and the use of the multifetal reduction procedure (3). Currently, most ART centres are reducing the number of embryos per transfer to one or two embryos to avoid high-order multiple pregnancies. However, triplet or high-order multiple pregnancies still occur because of the use of ovulation-induction drugs either alone or in combination with intrauterine insemination or as a result of monozygotic twins after the transfer of only two embryos. The last IVF world report (4) indicated that multifetal reduction was practised in 25 countries, and 236,661 cycles of intrauterine insemination were performed in 2010. The American College of Obstetrics and Gynecologists (ACOG) recommended that physicians should be knowledgeable regarding the multifetal reduction procedure and be required to provide patients with information, intervention, or both in a professional, ethical manner (3).

The aim of this work was to study and characterise multifetal reduction embryonic cells (MFR-ECs) aspirated from multifetal reduction of high-order multiple pregnancies.

3. MATERIALS AND METHODS

3.1. Materials

3.1.1. Reagents

- 2% Gelatin (Sigma-Aldrich, St. Louis, Missouri, USA).
- DMEM low glucose (Lonza, Walkersville, Maryland USA).
- FBS (Sigma, St. Louis, Missouri, USA).
- L-Glutamine (Lonza, Walkersville, Maryland, USA).
- Penicillin streptomycin amphotericin (Lonza, Walkersville, Maryland, USA).
- PureLink® RNA Mini Kit (Thermo Fisher Scientific, Waltham, Massachusetts, USA).
- High-Capacity cDNA Reverse Transcription Kit (Thermo Fisher Scientific, Waltham, Massachusetts, USA).
- GoTaq® DNA polymerase (Promega, Fitchburg, Wisconsin, USA).
- SsoAdvanced™ Universal SYBR® Green Supermix (Bio-Rad, Hercules, California, USA).
- Anti-Oct 4 (Cell Signaling Technologies, Beverly, Massachusetts, USA).
- ProLong gold antifade mountant (Molecular probes, Oregon, USA).
- PicoPlex whole genome amplification (WGA) Kit (Rubicon Genomics Inc., CAT. NO. R30050, Ann Arbor, Michigan, USA).
- NUDE mice (Swiss Nu/Nu, Charles River Laboratories, Paris, France).

3.1.2. Equipment and software

- CFX96 Touch™ Real-Time PCR Detection System (Bio-Rad, Hercules, California. USA).
- ChemiDoc™ Imaging System (Bio-Rad, Hercules, California, USA).
- Nikon A1R inverted laser scanning confocal microscope (Nikon microsystems, Massy, France).
- Microarray laser scanner (InnoScan 710) (Innopsys, Parc d'Activités Activestre, Carbonne, France).
- ChromoScreen software (IBSA Genetics) (Via del Piano, Lugano, Switzerland).

3.2. Methods

3.2.1. Multifetal reduction

The multifetal reduction procedure has been practised for more than two decades and has been approved by several ethical committees (2, 3, 5). In this protocol, couples with high-order multiple pregnancies (triplets or more) were counselled and signed an informed consent form. The procedure was performed at 6-7 weeks of gestational age corresponding to 4-5 weeks of embryonic development (6). IRB approval from the Faculty of Medicine Alexandria University, Egypt, Ethics Committee and informed consent from patients were obtained to use the tissue in research.

The procedure was performed under light general anaesthesia in the form of intravenous induction with propanol 2 mg/kg body weight, followed by inhalation of isoflurane 1.5.% and oxygen 100% through a face mask. The vagina was disinfected with povidone iodine 10% and then rinsed with saline solution. A transvaginal ultrasonic probe (7.5. MHZ) with a needle guide was introduced into the vagina. The number of gestational sacs with pulsating foetal echoes was visualised and confirmed. The needle was introduced through the needle guide into the vaginal vault and uterine wall and then into the lowest and most accessible gestational sac. The ultrasonically visible needle tip was directed towards the fetal echo, and suction was applied. The aspirated fetal tissues came through the needle in a closed system into a sterile tissue culture

Table 1. The sequence of primers used in RT-PCR

Gene Name	Forward	Reverse
Human β-actin	AGAGCTACGAGCTGCCTGAC	AGCACTGTGTTGGCGTACAG
Human FOXA2	CCGTTCTCCATCAACAACCT	GGGGTAGTGCATCACCTGTT
Human AFP	AGCAGCTTGTTAAATCAACATGCA	AAAATTAACTTTGGTAAACTTCTGACTCAGT
Human SOX17	CGCTTTCATGGTGTGGGCTAAGGACG	TAGTTGGGGTGGTCCTGCATGTGCTG
Human βIII-tubulin	GCTCAGGGGCCTTTGGACATCTCTT	TTTTCACACTCCTTCCGCACCACATC
Human GFAP	AGAAGCTCCAGGATGAAACC	AGCGACTCAATCTTCCTCTC
Human PAX6	TGGTATTCTCTCCCCCTCCT	TAAGGATGTTGAACGGGCAG
Human α-SMA	CCGACCGAATGCAGAAGGA	ACAGAGTATTTGCGCTCCGAA
Human MSX1	CCTCTTTGCTCCCTGAGTTCA	GGGACTCTTCCAGCCACTTTTT
Human CDK4	TCGAAAGCCTCTCTTCTGTG	TACATCTCGAGGCCAGTCAT
Human TP53	GTTCCGAGAGCTGAATGAGG	TTATGGCGGGAGGTAGACTG
Human SMAD7	AGAAGGTGCGGAGCAAAAT	GTGTGGCGGACTTGATGA
Human HER2	ATCTGCCTGACATCCACG	GCAATCTGCATACACCAGTTC

tube. The patient was observed after recovery from anaesthesia for 2 hours and then discharged from the hospital. Aspirated embryonic tissues were divided into four parts. The first part was placed in 25 µL phosphate buffered saline (PBS) to be used for cytogenetic analysis. The second part was fixed in 10% formaldehyde and embedded in paraffin blocks for histological and immunohistochemical analysis. The third part was used for *in vitro* tissue culture and further testing, while the fourth part was used for *in vivo* transplantation under the kidney capsule of immunodeficient NUDE mice.

3.2.2. Tissue culture

MFR-ECs were cultured in 2% gelatine-coated Petri dishes (Sigma-Aldrich) After 3 hours of tissue attachment, DMEM low glucose (Lonza) supplemented with 10% FBS (Sigma), 1% L-Glutamine (Lonza) and 1% penicillin streptomycin amphotericin (Lonza) was added and cultured at 37°C in 5% CO2 in an air humidified chamber. After 24 hours, cells were passaged by gentle scraping into uncoated Petri dishes (passage zero, the media was changed every three days). Cell passaging was performed when cells reached 70-80% confluence.

3.2.3. RNA extraction and RT-PCR

Total RNA was extracted from cells at day 0 and day 15 using a PureLink® RNA Mini Kit (Thermo Fisher Scientific). Total RNA was reverse-transcribed into cDNA using a High-Capacity cDNA Reverse Transcription Kit (Thermo Fisher Scientific). Samples were amplified using either GoTaq® DNA polymerase (Promega) for gel electrophoresis studies or SsoAdvanced™ Universal SYBR® Green Supermix (Bio-Rad) on a CFX96 Touch™ Real-Time PCR Detection System (Bio-Rad). Relative gene expression was normalised to the β-actin gene and calculated using the $2^{-\Delta\Delta CT}$ method. For gel electrophoresis, PCR products were run on 1% agarose and imaged using a ChemiDoc™ Imaging System (Bio-Rad, Hercules). The sequences of primers used are indicated in Table 1.

3.2.4. Confocal Immunofluorescence Imaging

Cells (on day 5) were grown for 24 hours on coverslips and then fixed with 4% paraformaldehyde, permeabilized with 0.1% Triton X-100, and blocked with 4% BSA. They were then stained with anti-Oct 4 (Cell Signaling Technologies) and labeled with the appropriate secondary antibody. Hoechst 33342 was used to visualize the nucleus and the cells were mounted using ProLong gold antifade mountant (Molecular probes). Cells were imaged using 60X objective of Nikon A1R inverted laser scanning confocal microscope (Nikon microsystems).

3.2.5. Histology and immunohistochemistry

Fresh tissues on day 0 were washed to remove blood from the operational procedures. Cells were harvested using cell scrapers at different time points (day 5 and day 15). Samples from the different time points (fresh tissues at day 0, day 5, and day 15) were fixed in 10% formaldehyde for 24 hours at room temperature. Paraffin blocks were prepared, and 5-µm-thick sections were subjected to histological and histochemical studies. Histological studies used haematoxylin and eosin (HE) to demonstrate the histological structure (7). Histochemical studies applied safranin O staining to detect proteoglycans and chondrocyte differentiation, the PAS reaction for glycogen content and hepatic differentiation, and Luxol fast blue-periodic acid Schiff (LFB-PAS) staining to recognise myelin basic protein. Silver impregnation was used for neurofibrils, and both LFB-PAS and silver impregnation were used to detect neural progenitors. For immunohistochemistry analysis, sections from day 0 were immunostained for desmin, S-100, chromogranin and synaptophysin using a Ventana Bench Mark GX autostainer (Ventana ultraView DAB Detection System).

Table 2. Morphometric results

Duration in days	Mean count of cells	Mean area of Safranin O cells	Mean area of ECM	Mean area of PAS +ve cells	Mean area of LFB +ve myelin basic protein
0	5.7±0.1	3.6.4±0.2.	–	2.9.8±0.3	–
5	19.3±3.4.1	14.3.1±3.2.1	5.0.1±1.3	10.5.5±2.4.1	9.2.2±1.9
15	37.8±4.9.2	35.7.6±5.1.2	18.2±3.2.3	32.8.9±4.5.2	36.9.9±5.2.3

[1]Significant compared to day 0, [2]Significant compared to day 0 and day 5, [3]significant compared to day 5
Mean count of cells, area (μ_2) of Safranin O +ve cells, area of ECM, area of PAS +ve cells and area of LFB +ve myelin basic protein

3.2.6. Morphometric studies

Using a computer-assisted image analysis system, assessment of the quantification of cells, area (μm2) of safranin O-positive cells, area of extracellular matrix (ECM), area of PAS-positive cells and area of LFB-positive myelin protein were performed in HE-, safranin O-, PAS- and LFB-PAS-stained sections using an interactive measurement menu. Measurements were performed in 10 high-power fields. Quantitative data were summarised as the means and standard deviations and compared using one-way analysis of variance (ANOVA). Significant ANOVA was followed by Bonferroni post hoc tests to detect which pairs of groups caused the significant difference. P-values <0.0.5 were considered significant. Calculations were made using Statistical Package for the Social Sciences (SPSS) version 16 (8) (Table 2).

3.2.7. Cytogenetic analysis

A PicoPlex whole genome amplification (WGA) Kit (Rubicon Genomics Inc.) was used to lyse the tissue in PBS and amplify DNA to obtain enough material for genetic analysis with a DNA array for aneuploidy screening. The ChromoScreen protocol was performed where amplified DNA (green) was tested with reference DNA (red). Purification and precipitation of the product mix were followed by dissolving the DNA pellet in hybridisation buffer. The dissolved labelled DNA was desaturated at 75°C and dropped into the array slide, covered with a coverslip and hybridised overnight at 47°C. The array slide was washed and scanned with a microarray laser scanner (InnoScan 710) (Innopsys). Scanned images were analysed by ChromoScreen software (IBSA Genetics). This technique is a comparative genomic hybridization (CGH) microarray.

3.2.8. *In vivo* transplantation

All animal procedures were carried out in the Urology and Nephrology Center Animal House in accordance with the institutional and National Institutes of Health Guidelines for the Care and Use of Laboratory animals. NUDE mice (Swiss Nu/Nu, Charles River Laboratories, Paris, France) were housed with one mouse per cage. Mice were anesthetized by intraperitoneal injection of ketamine (100 mg/kg) and diazepam (5 mg/kg). A total of 1 × 106 cells were implanted under the kidney capsule. After 7 weeks, the mice were euthanized, and the kidneys were fixed with PBS containing 4% paraformaldehyde. Paraffin-embedded tissue was sliced and stained with HE for histological analysis.

4. RESULTS

4.1. Histology and immunohistochemistry

HE staining on day 0 showed a mixture of differentiated cells. These cells included cerebellar neural tissue (Figure 1A) and tubular structures with pseudostratified columnar ciliated epithelium (possibly respiratory) surrounded by primitive mesenchyme (Figure 1B), as well as primitive striated muscle cells (rhabdomyoblasts, Figure 1C). Other structures included sheets of primitive mesenchymal cells surrounding thin-walled blood capillaries (Figure 1D); papillary structures covered by simple squamous epithelium, which continues into columnar epithelium, covering a stromal core of vascular primitive mesenchyme (Figure 1E); and chorionic villi and foetal membranes (Figure 1F and 1G). Samples from day 5 demonstrated an increase in the cellular density of pleomorphic cells (Figure 1H and 1I). On day 15, there was a further increase in cellular density with the appearance of pleomorphic cells (Figure 1J and 1K).

Immunohistochemistry showed positive focal staining for desmin, S-100 protein, synaptophysin and chromogranin on day 0. Desmin-positive immunoreactivity was detected in primitive muscle cells (Figure 2A), primitive mesenchymal cells and myoepithelial cells (Figure 2B), and spindle-shaped cells in the core of chorionic villi (Figure 2C). S-100 immunoreactivity was positive in cartilage cells (Figure 2D), cells with a neuroectodermal origin (Figure 2E), and cerebellar tissue (Figure 2F). Synaptophysin was positive in neuroectodermal cells and brain tissue (Figure 2G, 2H, 2I). Chromogranin was positive in cells of neuroectodermal origin (Figure 2J, 2K) and negative in chorionic villi (Figure 2L).

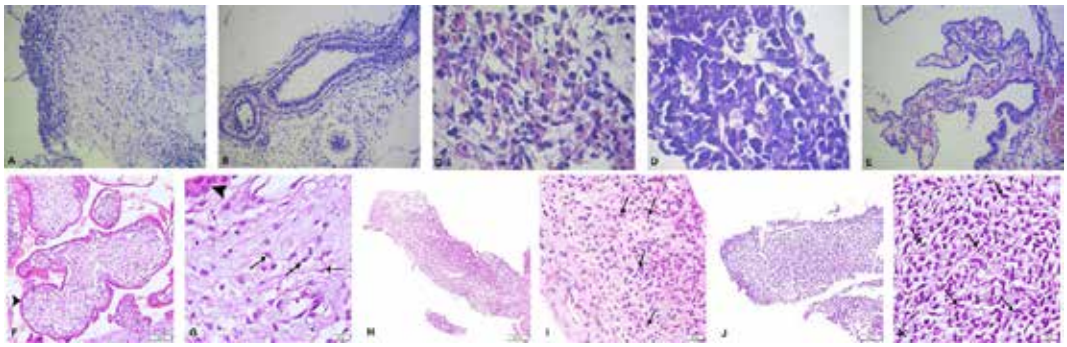

Figure 1. Histological analysis of MFR-ESCs. (A) Cerebellar neural tissue (HE x100), (B) respiratory epithelium (HE x100), (C) rhabdomyoblasts (HE x100), (D) primitive mesenchymal cells surrounding thin-walled blood capillaries (HE x100), (E) simple squamous epithelium, columnar epithelium and vascular primitive mesenchyme. (F) Day 0 showing chorionic villi covered by trophoblastic cells (arrowhead) (HE x100), and (G) a few spindle cells (arrows) exhibiting flattened nuclei and surrounded by extracellular matrix. The trophoblastic epithelium (arrowhead) (HE x400), (H) day 5 sample showing increased cellular density, (I) higher magnification of the previous Figure showing multiple pleomorphic cells (arrows) (HE x400), (J) day 15 sample showing an obvious increase in the cellular density (HE x100), (K) higher magnification of the previous image showing numerous pleomorphic cells (arrows) (HE x400)

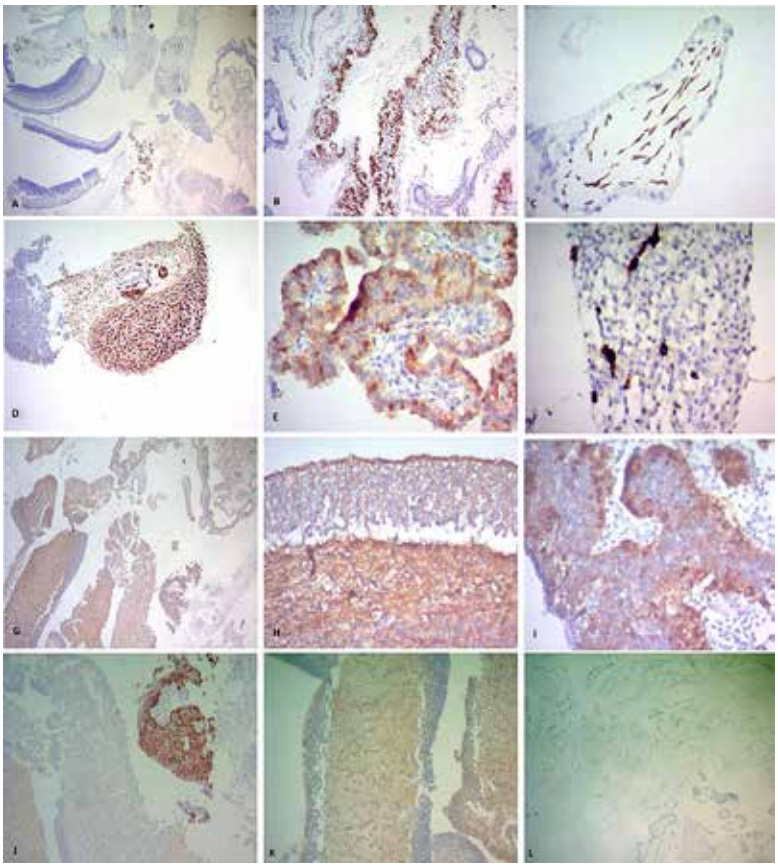

Figure 2. Immunohistochemistry studies of MFR-ESCs. Desmin positivity in (A) rhabdomyoblasts (X 40), (B) myoepithelial cells (x100), (C) chorionic villi (x400). Positive S-100 in (D) cartilage cells (x100), (E) choroid plexus neuroectodermal cells (x100), (F) cerebellar tissue (x400). Synaptophysin positivity in (G) neuroectodermal cells and brain tissue fragments (x40), (H) brain tissue (x400), (I) neuroectodermal cells (x400). Chromogranin positivity in: (J) cells of neuroectodermal origin (x200), (K) cerebellar tissue (x200), (L) chorionic villi negative for chromogranin (x40).

4.2. Histochemical analysis

Using Safranin O to detect chondrocyte differentiation, samples from day 0 showed few positively stained cells but negatively stained ECM (Figure 3A). On day 5, multiple cells positively stained for chondrogenic lineage markers were observed with minimal staining of ECM (Figure 3B). However, on day 15, the number of positively stained cells was significantly increased with obvious staining of

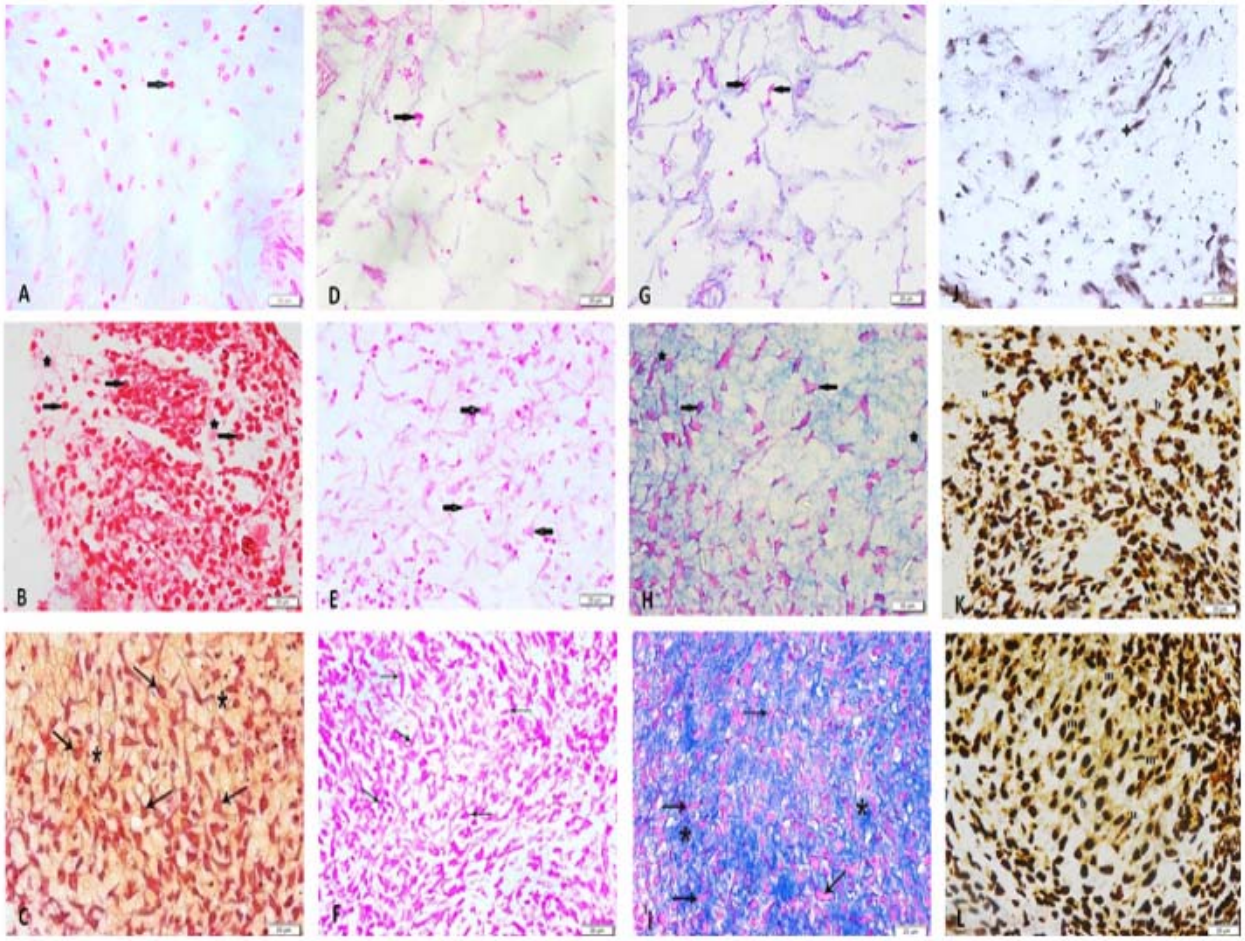

Figure 3. Histochemical studies of cultured MFR-ESCs. (A-C) Safranin O stain, proteoglycans and chondrocyte differentiation stain showing cells of chondrogenic origin at day 0 (a), day 5 (b) and day 15 (c). (D-F) PAS staining, glycogen and hepatic differentiation staining showing a positive reaction in cells of the hepatic lineage at day 0 (d), day 5 (e), and day 15 (f). (G-I) LFB-PAS staining, neural lineage differentiation staining at day 0 (g), day 5 (h) and day 15 (i). (J-L) Silver impregnation staining, neural lineage differentiation staining: (J) day 0 sample showing no staining of a few spindle cells (asterisks), (K) day 5 positive staining of unipolar (u) and bipolar (b) cells, (L) day 15 positive staining of multipolar (m), bipolar (b) and unipolar (u) cells.

the ECM. This finding was confirmed by a significant increase in the mean area of Safranin O-positive ECM. (Figure 3C). These data showed that chondrogenic proteoglycan content was increased. As deposition of cartilage-specific proteoglycans established the chondrogenic potential of cultured cells, these cells could indeed provide an immensely valuable source of chondrocytes. Details regarding morphometric studies are provided in Table 2.

PAS staining was used to examine the hepatic differentiation capacity of these embryonic cells. Samples from day 0 demonstrated a PAS-positive reaction in the cytoplasm of a few cells (Figure 3D). On day 5, a PAS-positive reaction was detected in the cytoplasm of multiple pleomorphic cells (Figure 3E). The number of PAS-positive pleomorphic cells was significantly increased on day 15 (Figure 3F). This glycogen storage capacity suggested the acquisition of hepatic function. LFB-PAS staining of samples from day 0 showed positive PAS staining in a few cells and negative staining of myelin basic protein (Figure 3G). Day 5 samples showed obvious staining of myelin basic protein, and a PAS-positive reaction was observed in the cytoplasm of multiple pleomorphic cells (Figure 3H). On day 15, extensive staining of myelin basic protein and a PAS-positive reaction were detected in the cytoplasm of numerous pleomorphic cells (Figure 3I). This result was confirmed by a significant increase in the mean area of LFB-positive myelin protein in the ECM, verifying the ability of these embryonic cells to differentiate into neural progenitors in culture.

By silver impregnation, samples from day 0 showed negative staining of a few spindle cells (Figure 3J). Day 5 showed positive staining of some unipolar and bipolar cells (Figure 3K). On day 15, multiple nerve-like multipolar cells with positive staining were recognised (Figure 3L). Thus, these cells can be considered a reliable source for neural progenitors, overcoming the challenges that face neural induction processes.

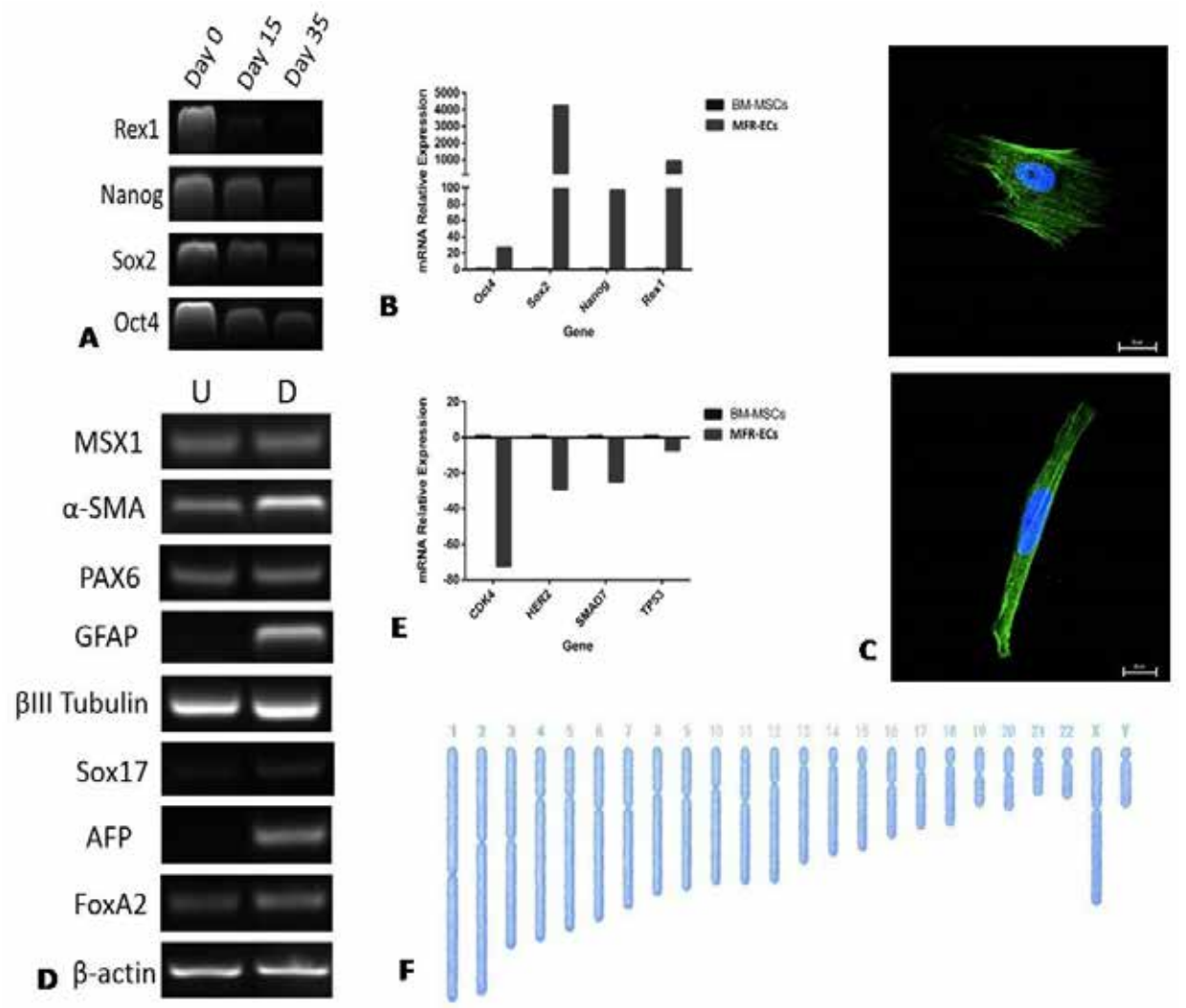

Figure 4. RT-PCR (A), and qPCR (B) analysis of MFR-ECs for OCT4, NANOG, SOX2 and REX-1 markers. (C) Confocal microscopy image confirms positive expression of Oct4 (green). Nuclei (Blue) were stained using Hoechst 33342. (D) Differentiation markers for the three germ layers using RT-PCR analysis of at day 0 and day 15. (E) Cancer-related markers CDK4, SMAD7, and HER2 were down-regulated in MFR-ECs in compared with hBM-MSCs at day 0. (F) Comparative genomic hybridization of the aspirated fetal cells showing normal male karyotype.

4.3. Expression of genes related to the three germ layers

RT-PCR analysis at day 0 and day 15 confirmed that these differentiated cells expressed markers of all three germ layers, which included important developmental transcription factors such as beta three-tubulin (βIII-tubulin, ectoderm), forkhead box A2 (FOXA2, endoderm), paired box 6 (PAX6, ectoderm), alpha-smooth muscle actin (α-SMA, mesoderm) and Mshhomeobox 1 (MSX1, mesoderm). The markers that showed a substantial increase were α-fetoprotein (AFP, endoderm), glial fibrillary acidic protein (GFAP, ectoderm) and SRY-box-containing gene 17 (SOX17, endoderm) (Figure 4D). Furthermore, expression of mRNAs encoding OCT4, NANOG, SOX2 and REX-1 observed at day 0 was gradually downregulated when the cells were cultured in media containing 10% FBS, as observed on day 15, and on day 35 (Figure 4A). Significantly higher expression of mRNAs encoding OCT4, NANOG, SOX2 and REX-1 was observed in MFR-ECs at day 0, compared to human bone marrow mesenchymal stem cells (hBM-MSCs, Figure 4B).. Furthermore,, MFR-ECs were positive for Oct4 expression as shown by confocal immunofluorescence imaging (Figure 4C).

4.4. Low expression levels of cancer-related genes

qPCR analysis was used to investigate the expression of cancer-related genes in embryonic cells. Our data showed down-regulation of the mRNAs of

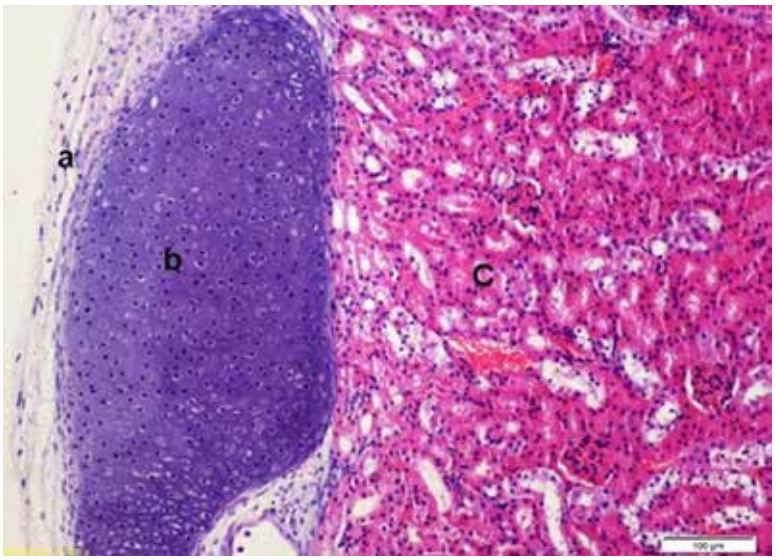

Figure 5. In vivo transplantation of MFR-ESCs. Histological analysis using HE seven weeks after transplantation of MFR-ESCs under the kidney capsule of immunodeficient nude mice showing a plate of hyaline cartilage with a typical (a) perichondrium, (b) chondrocytes in lacunae, and homogenous matrix. The mouse renal cortex (C).

cancer-related genes, including CDK4, SMAD7 and HER2, in MFR-ECs compared with those in human bone marrow-derived mesenchymal stem cells (hBM-MSCs) at day 0. Of special interest, TP53, which has been demonstrated as an inhibitor of pluripotency, was also down-regulated (Figure 4E). Furthermore, our cytogenetic analysis using a CGH microarray showed that MFR-ECs had a normal karyotype (Figure 4F).

4.5. *In vivo* transplantation

Histological analysis using HE seven weeks after transplantation of embryonic cells under the kidney capsule of immunodeficient NUDE mice showed a plate of typical hyaline cartilage with perichondrium (Figure 5A) and chondrocytes in lacunae (Figure 5B) in a homogenous matrix.

5. DISCUSSION

Using histology and immunohistochemistry, we demonstrated that embryonic cells aspirated during a multifetal reduction procedure contained a mixture of cells at different stages of differentiation. These cells increased in density as they vigorously proliferated as demonstrated from samples taken on days 5 and 15 in culture. MFR-ECs contained differentiated cells from the three germ layers, the ectoderm, mesoderm, and endoderm. Lineage-specific markers, such as neural and hepatic lineages, increased with time in culture. The cells had a normal karyotype and did not express cancer-related genes. Furthermore, upon transplantation under the kidney capsule, they did not form teratoma, which typically develop following injection of blastocyst-derived embryonic stem cells. Our data showed that MFR-ECs contain cells of chondrogenic origin, which can deposit chondrogenic proteoglycans, unlike mesenchymal stem cells (MSCs), which failed to secrete weight-bearing hyaline articular cartilage (9). Of special interest, MFR-ECs contained cells of hepatogenic lineage. Current protocols used for the differentiation of MSCs into hepatic lineage cells are expensive, time-consuming and include several complicated steps (10-13). Other cells, such as induced pluripotent stem cells (iPSCs), were induced for hepatocyte differentiation but failed to give rise to fully mature hepatocytes, resulting in a heterogeneous population (14, 15). In contrast, MFR-ECs spontaneously differentiated into hepatic cells in culture. Similarly, MFR-ECs differentiated into cells with a neural phenotype as shown by histology and immunohistochemistry. Thus, these cells represent a physiologically relevant model for stem cell expansion and differentiation.

The embryonic cells described in this report were obtained from ethically approved and clinically discarded embryonic tissues at 4-5 weeks of development (6). The product of conception from implantation until the eighth week of development is considered an embryo, and from the ninth week to birth, it is called a fetus (16). Embryonic tissues at this stage of development are a rich source of functionally differentiated cells that maintain rigorous proliferative capacities. After the third week of embryo development, the three germ layers, the ectoderm, endoderm, and mesoderm, are formed and start to give rise to the primordia of all tissues and organs (17). This period of development is characterised by the upregulation of differentiation transcriptional factors (18). MFR-ECs showed expression of OCT4,

NANOG, SOX2 and REX-1 markers at day 0, which decreased with time at day 15 and day 35. These data were paralleled with upregulation in the lineage specific markers, confirming that MFR-ECs maintain early broader differentiation potential. When MFR-ECs were transplanted under the kidney capsule of NUDE mice, they formed a typical plate of hyaline cartilage tissue and did not form a teratoma. This finding indicates that these cells do not share the teratogenic characteristics of embryonic stem cells collected from day 3-7 blastocysts (19). The lack of *in vivo* teratoma formation is consistent with this stage of development at week 4, which is the beginning of organogenesis (20-21). At this stage, differentiation programming proceeds at different rates for different tissues, accounting for the detection of a mixture of cells and stage-specific differentiation markers. However, none of the remaining cells maintain the pluripotent potential of blastocyst-derived embryonic stem cells that characterise *in vivo* teratoma formation.

In conclusion, we reported that MFR-ECs represent a rich source of stage-specific, functionally differentiated cells that could be used as a valuable *in vitro* model to study the process of stem cell development and differentiation. MFR-ECs could also serve as an excellent, unique model to study the embryological and physiological development of tissues of neural, chondrogenic, hepatic and other lineages.

6. ACKNOWLEDGEMENTS

We thank Professor M. Ghoneim for the research facilities at Mansoura University Urology and Nephrology Center. This work was supported by grant #5300, funded by the Scientific and Technology Development Fund (STDF), Egypt. The authors have no conflicts of interest related to this work.

7. REFERENCES

1. J. A. Martin, B. E. Hamilton, S. J. Ventura, M. J. Osterman, E. C. Wilson and T. J. Mathews: Births: final data for 2010. *Natl Vital Stat Rep*, 61(1), 1-72 (2012)

2. Multiple gestation associated with infertility therapy: an American Society for Reproductive Medicine Practice Committee opinion. *Fertil Steril*, 97(4), 825-34 (2012)
DOI: 10.1016/j.fertnstert.2011.11.048

3. ACOG Committee Opinion No. 553: Multifetal Pregnancy Reduction. *Obstetrics & Gynecology*, 121(2), 405-410 (2013)
DOI: 10.1097/01.AOG.0000426426.71962.2a

4. S. Dyer, G. M. Chambers, J. de Mouzon, K. G. Nygren, F. Zegers-Hochschild, R. Mansour, O. Ishihara, M. Banker and G. D. Adamson: International Committee for Monitoring Assisted Reproductive Technologies world report: Assisted Reproductive Technology 2008, 2009 and 2010. *Hum Reprod*, 31(7), 1588-609 (2016)
DOI: 10.1093/humrep/dew082

5. Multiple gestation pregnancy. The ESHRE Capri Workshop Group. *Hum Reprod*, 15(8), 1856-64 (2000)
DOI: 10.1093/humrep/15.8.1856

6. R. T. Mansour, M. A. Aboulghar, G. I. Serour, M. A. Sattar, A. Kamal and Y. M. Amin: Multifetal pregnancy reduction: modification of the technique and analysis of the outcome. *Fertility and Sterility*, 71(2), 380-384 (1999)
DOI: 10.1016/S0015-0282(98)00461-0

7. K. Zbigniew: J.A. Kiernan. Histological and Histochemical Methods: Theory and Practice. 5th edition, Scion Publishing, 2015, 571 pp. J.A. Kiernan. Histological and Histochemical Methods: Theory and Practice. 5th edition, Scion Publishing, 2015, 571 pp., 54(1), 58-59-58-59 (2016)

8. R. Emsley, G. Dunn and I. R. White: Mediation and moderation of treatment effects in randomised controlled trials of complex interventions. *Stat Methods Med Res.*, 19(3), 237-270 (2009)
DOI: 10.1177/0962280209105014

9. R. Somoza, J. F Welter, D. Correa and A. I Caplan: Chondrogenic Differentiation of Mesenchymal Stem Cells: Challenges and Unfulfilled Expectations. *Tissue Eng Part B Rev.* (2014)
DOI: 10.1089/ten.TEB.2013.0771

10. Q. Li, A. P. Hutchins, Y. Chen, S. Li, Y. Shan, B. Liao, D. Zheng, X. Shi, Y. Li, W.-Y. Chan, G. Pan, S. Wei, X. Shu and D. Pei: A sequential EMT-MET mechanism drives the differentiation of human embryonic stem cells towards hepatocytes. *Nat Commun.*, 8, 15166 (2017)
DOI: 10.1038/ncomms15166

11. D. Campard, P. A. Lysy, M. Najimi and E. M. Sokal: Native Umbilical Cord Matrix Stem Cells Express Hepatic Markers and Differentiate into Hepatocyte-like Cells. *Gastroenterology*, 134(3), 833-848 (2008)
DOI: 10.1053/j.gastro.2007.12.024

12. T. Tamagawa, S. Oi, I. Ishiwata, H. Ishikawa and Y. Nakamura: Differentiation of mesenchymal

cells derived from human amniotic membranes into hepatocyte-like cells *in vitro*. *Hum Cell.* (2007) DOI: 10.1111/j.1749-0774.2007.00032.x

13. Y.-N. Zhang, P.-C. Lie and X. Wei: Differentiation of mesenchymal stromal cells derived from umbilical cord Wharton's jelly into hepatocyte-like cells. *Cytotherapy*, 11(5), 548-558 (2009) DOI: 10.1080/14653240903051533

14. A. Carpentier, I. Nimgaonkar, V. Chu, Y. Xia, Z. Hu and T. J. Liang: Hepatic differentiation of human pluripotent stem cells in miniaturized format suitable for high-throughput screen. *Stem Cell Res*, 16(3), 640-650 (2016) DOI: 10.1016/j.scr.2016.03.009

15. S. Snykers, J. De Kock, V. Rogiers and T. Vanhaecke: *In vitro* Differentiation of Embryonic and Adult Stem Cells into Hepatocytes: State of the Art. *STEM CELLS*, 27(3), 577-605 (2009) DOI: 10.1634/stemcells.2008-0963

16. T. Ishii and K. Eto: Fetal stem cell transplantation: Past, present, and future. *World J Stem Cells*, 6(4), 404-420 (2014) DOI: 10.4252/wjsc.v6.i4.404

17. K. L. Moore, T. V. N. Persaud and M. G. Torchia: Before we are born: essentials of embryology and birth defects. Philadelphia, (2008)

18. H. Yi, L. Xue, M.-X. Guo, J. Ma, Y. Zeng, W. Wang, J.-Y. Cai, H.-M. Hu, H.-B. Shu, Y.-B. Shi and W.-X. Li: Gene expression atlas for human embryogenesis. *FASEB J,* 24(9), 3341-3350 (2010) DOI: 10.1096/fj.10-158782

19. J. Cunningham, T. M. Ulbright, M. Pera and L. Looijenga: Lessons from human teratomas to guide development of safe stem cell therapies. *Nat Biotechnol*. 30, 849, 2012 (2013).

20. Y. R. Barishak: Embryology of the eye and its adnexa. Karger Medical and Scientific Publishers, (2001) DOI: 10.1038/nbt.2329

21. F. Müller and R. O'Rahilly: The development of the human brain from a closed neural tube at stage 13. *Anatomy and embryology*, 177(3), 203-224 (1988) DOI: 10.1007/BF00321132

Key Words: Embryonic Stem Cells, Multifetal Reduction, Progenitor Cells

Send correspondence to: Nagwa El-Badri, Biomedical Sciences Program, Director, Center of Excellence, for Stem cells and Regenerative Medicine (CESC), Zewail City of Science and Technology, Ahmed Zewail Road, October Gardens, 6th of October City, Giza, Egypt, Building: Helmy Institute of Biomedical Sciences, Room number: F010, Egypt, Tel: 20238540401, Fax: 20 238540401, E-mail: nelbadri@zewailcity.edu.eg.